



## Bulk synthesis route of the oriented arrays of tip-shape ZnO nanowires and an investigation of their sensing capabilities

Mashkoor Ahmad<sup>a</sup>, Caofeng Pan<sup>a</sup>, Javed Iqbal<sup>b</sup>, Lin Gan<sup>a</sup>, Jing Zhu<sup>a,\*</sup>

<sup>a</sup> Beijing National Center for Electron Microscopy, The State Key Laboratory of New Ceramics and Fine Processing, Laboratory of Advanced Material, China Iron & Steel Research Institute Group, Department of Material Science and Engineering, Tsinghua University, Beijing 100084, China

<sup>b</sup> Laboratory of Advanced Materials, Department of Material Science and Engineering, Tsinghua University, Beijing 100084, China

### ARTICLE INFO

#### Article history:

Received 7 July 2009

In final form 26 August 2009

Available online 31 August 2009

### ABSTRACT

Bulk tip-shape ZnO nanowires (TSZONWs) have been synthesized via thermal evaporation method. The carbon nanotubes have been found to play an important role for the synthesis of this structure. The sensing capabilities of the structures have been investigated through electrochemical measurements. The photoluminescence spectra exhibit strong visible emission band due to an increase amount of defects, which leads to a significant role in the sensing applications. The electrochemical measurements prove that the TSZONWs are very sensitive to the pH of the PB solution as well as the bio-chemical species. Our investigation demonstrates that the arrays of TSZONWs can be employed for various applications.

© 2009 Elsevier B.V. All rights reserved.

### 1. Introduction

Zinc Oxide is a versatile semiconductor material with a wide direct band gap of 3.3 eV, which has been found useful in many applications such as opt-electronic devices, surface acoustic wave devices, field emitters, piezoelectric, transparent conducting materials and solar cells [1–7]. In addition it has been effectively used as a gas and chemical sensor material based on the near-surface modification of charge distribution with certain surface-absorbed species [8–11]. On the other hand, ZnO is attracting considerable attention due to their unique ability to form a variety of nanostructures with different morphologies. Under specific controlled growth conditions, arrays of ZnO nanowires have been deposited on various substrates [12,13] and different nanostructures such as nanocombs, nanorings, nanobelts, nanowires and nanocages have been synthesized [14,15]. Among different morphologies oriented ordered arrays of tip-shape ZnO nanowires have their significant applications such as field emission, scanning probing microscopy (SPM) and highly sensitive sensing devices. Since the discovery of carbon nanotubes (CNTs) by Iijima [16], these nanostructures can be used as substrate [17] for the controlled fabrication of different nanostructures. Kim et al. used a heat-treating method for a mixture of Zn/CNT to obtain ZnO nanowires [18]. Recently, Chrissanthopoulos et al. used ZnO/graphite/CNTs to obtain ZnO nanostructures [19].

Besides, ZnO nanorods, nanowires and nanotubes have been employed for the detection of biological molecules [20–25]. Among a variety of nanosensor systems, pH sensor miniaturization is

highly important, since the large surface-to-volume ratio leads to a short diffusion distance of the analyte towards the electrode surface, thereby providing an improved signal to noise ratio, faster response time, enhance analytical performance and increased sensitivity [26]. Although recently many works has been done on the ZnO nanostructures based biosensors [27–30], the ion sensitivity of the ZnO nanostructures in aqueous solution has not been systematically investigated so far. The detection sensitivity of the ZnO-NWs based pH sensor is achieved by monitoring minimal changes in electrochemical current response caused by binding of species on the surfaces of the ZnO-NWs. When a bio-chemical species emerges in a polar solvent, a surface charge will develop through one or more of the following mechanisms; preferential adsorption of ions; dissociation of surface charged species; isomorphic substitution of ions; accumulation or depletion of electrons at the surface; physical adsorption of charged species onto the surface. The polar or nonpolar surface structures of ZnO-NWs are of interest in understanding the mechanism of interaction of these surfaces with the medium surrounding them. The sensing mechanism for chemical adsorbates in piezoelectric materials originates from compensation of the polarization-induced bound surface charge by interaction with the polar molecules in the liquids [31]. Steinhoff et al. suggest that the native oxide on the nitride surface was responsible for the pH sensitivity of the response of gateless GaN-based heterostructure transistors to electrolyte solutions. The pH response of metal oxide surfaces has been modeled by a number of groups in terms of formation of hydroxyl groups that lead to a pH-dependent net surface change with a resulting change in voltage drop at the semiconductor/ liquid interfaces [32–35]. Ambacher et al. have shown a strong sensitivity of AlGaIn/GaN heterostructures to ions, polar liquids, hydrogen gas and even

\* Corresponding author. Fax: +86 10 62771160.

E-mail address: [jzhu@mail.tsinghua.edu.cn](mailto:jzhu@mail.tsinghua.edu.cn) (J. Zhu).

biological materials. In particular they have shown that it is possible to distinguish liquids with different polarities.

Among different approaches, the focus of current study is divided into two parts; firstly, the synthesis method of oriented arrays of tip-shape ZnO nanowires (TSZONWs) on MWCNTs coated Si substrate, Secondly, the investigation of sensing capabilities of these NWs for the pH as well as bio-chemical species via electrochemical measurements. The mechanism for detection is the change in current response as chemical species absorb on the ZnO nanostructures.

## 2. Experimental

### 2.1. Synthesis of ZnO nanostructures

Synthesis of ZnO nanostructures were carried out in a horizontal quartz tube furnace via thermal evaporation method, where the temperature, pressure and flow rates of working gases were well controlled. In a sample preparation steps, a solution was prepared by dissolving 1 mg multiwalls carbon nanotubes (MWCNTs) in 10 ml ethanol under stirring for 5 h. Two Si substrates were cleaned carefully, followed by supersonically in acetone, alcohol and de-ionized water for 30 min each and put a drop of prepared solution on one of them physically. The substrates were dried for 5 h at room temperature and then mounted downward region of the furnace where the temperature was about 500 °C. A crucible containing the metallic Zn powder (99.99% purity) was placed in the central region of the quartz tube furnace and heated to 700 °C for 3 h. Mixed gas (90% Ar, 10% O<sub>2</sub>) flows through the quartz tube at a rate of 180 sccm. The distance between Zn source and substrates was about 5 mm. After the reaction completed, the as-prepared products were examined by field emission scanning electron microscope (JEOL FESEM-6301F), high resolution transmission electron microscope (HRTEM-JEM-2011F), X-ray diffraction (XRD) and photoluminescence (PL).

### 2.2. Fabrication of modified electrode

For the measurements of sensing capabilities of the nanostructures, a conventional gold electrode (with 3 mm in diameter) was wetted by 0.1 M phosphate buffer solution (PBS) with pH 7.0 and the prepared nanostructures were transferred to gold electrode as shown in the schematic Fig. 4a. The as-prepared ZnO nanostructures/gold electrode was then dried in air for 2 h. A 5 µl of 0.25% polyvinyl alcohol (PVA) solution was dropped onto the ZnO-NWs/gold electrode and dried to form a film, which is critical to attach ZnO-NWs tightly on the surface of the gold electrode. Following the evaporation of water, subsequently, a 5 µl of 0.01 mol/L L-cysteine is dropped onto the surface of the PVA/ZnO-NWs/gold electrode via physical adsorption. The modified electrode (L-cysteine/PVA/ZnO-NWs/gold electrode) was kept at 4 °C in refrigerator overnight. The electrochemical experiments were performed at room temperature utilizing an electrochemical workstation (CHI660C) with a three electrodes mode, the modified gold electrode was used as the working electrode, with Hg/Hg<sub>2</sub>SO<sub>4</sub> as the reference electrode, and silver as the counter electrode. The pH of the solution was real-time measured by a pH meter.

## 3. Results and discussions

### 3.1. Material characterization

The structures of the as-grown products have been characterized by X-ray diffraction. Fig. 1 shows the XRD pattern of the both products grown on carbon nanotubes coated Si substrate and the

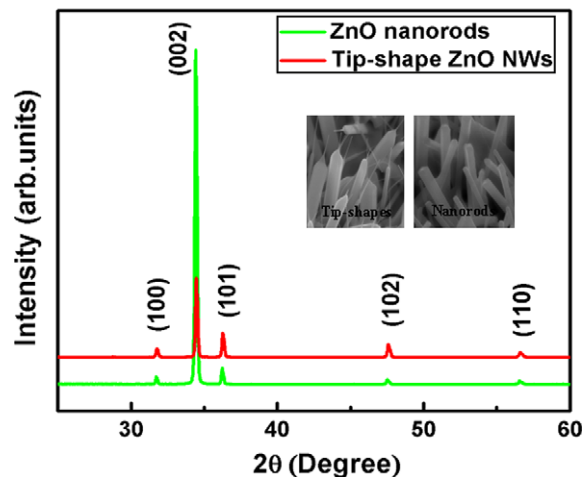
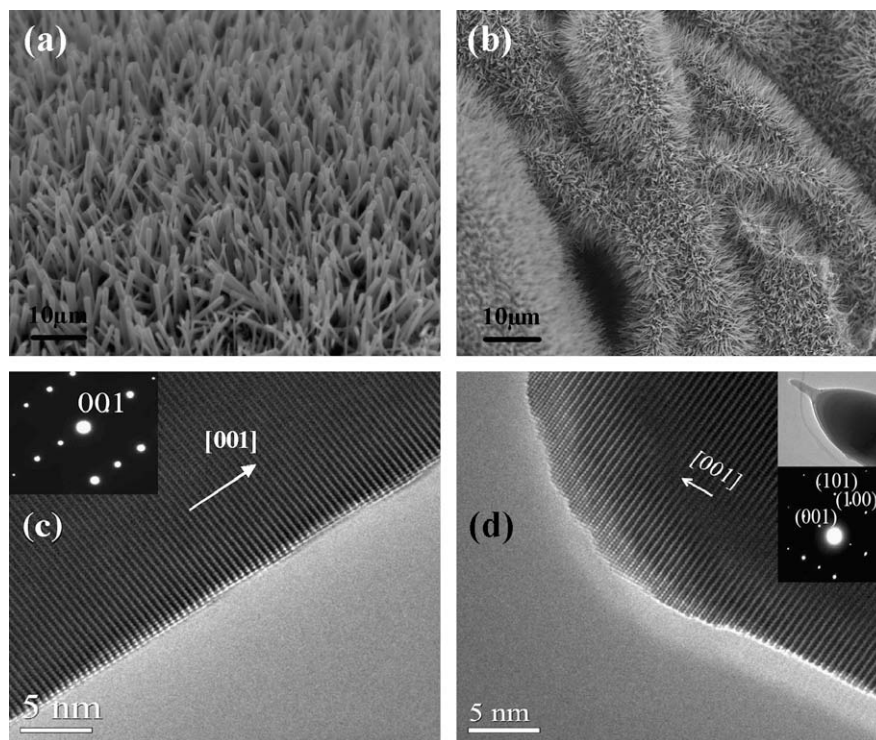


Fig. 1. XRD pattern of the as-grown products on carbon nanotubes coated Si substrate and bare Si substrate. Inset is the magnified SEM images of the both products.

bare Si substrate. It can be seen from the pattern that all major diffraction peaks exhibit a typical wurtzite hexagonal structure such as bulk ZnO. No additional peak is observed in the pattern due to the products in bulk form. The evaluated *c*-axis lattice constant is 0.5140 nm, which is same as that of the ZnO (*c* = 0.5109 nm). The insets Fig. 1 show the magnified SEM images of the both products.

The morphology of the as-grown products has been analyzed by employing FESEM. It has been revealed that the product on CNTs coated Si substrate consists of ordered arrays of oriented TSZONWs as shown in Fig. 2b. The length of each NW is in the range of 3–6 µm while the diameter is <10 nm at the top edge and 50–300 nm in the bottom region. The product on the bare Si substrate consists of nanorods with uniform diameter in the range of 150–400 nm and length in 5–8 µm as shown in Fig. 2a. The HRTEM image and selected area electron diffraction (SAED) pattern of individual isolated ZnO nanorod and TSZONW are shown in Fig. 2c and d. It is found that the nanostructures have single-crystalline nature and grown along the [0 0 1] directions. The corresponding SAED pattern is identical over the entire TSZONW and the nanorod. The lattice constant calculated from the SAED are 3.2652 Å for *a* and 5.2213 Å for *c*, which are also consistent with those of ZnO (*a* = 3.2535 Å, *c* = 5.2151 Å). The TEM image of the tip-shape ZnO NW is also recorded as shown in Fig. 2d inset.

Fig. 3 shows the PL spectra of the oriented TSZONWs and ZnO nanorods at room temperature. In the figure, the PL spectra consist of two parts: one narrow weak peak in the ultraviolet (UV) region and another broad emission band in visible light (VL) region. In the UV region, the emission peak is at about 378 nm, which is generally originated from the near-band-edge (NBE) exciton transition in wide band gap of ZnO, namely the recombination of free excitons through collision process [36]. In VL region, NWs exhibit broad green luminescence band in the range of 450–650 nm, which is usually related to the defects (such as oxygen vacancy, Zn interstitial) in ZnO structure, in which the emission results from the radiative recombination of photo-generated hole with an electron occupying the defect or oxygen vacancy [37]. The broad luminescence band illustrates the increase of defects in the tip-shape NWs. It has been also seen that the PL emission does not fall to zero between the UV and broad emission peaks, which indicates the presence of an additional transition in the range 400–450 nm. Emission in the blue spectral range for ZnO has been reported in the literature [38–41]. Possible candidate for transitions in this spectral range are zinc vacancy (405 nm), zinc interstitial



**Fig. 2.** (a) SEM image of oriented tip-shape ZnO nanowires. (b) SEM image of ZnO nanorods. (c) HRTEM image of ZnO nanorod; inset is the corresponding SAED. (d) HRTEM image of tip-shape ZnO nanowire; inset is the SAED and TEM image of tip-shape NW.

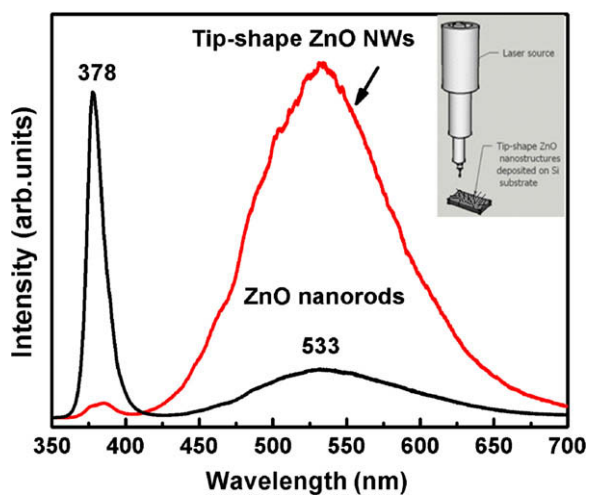


**Fig. 3.** Room temperature photoluminescence spectra of the nanostructures; inset is the schematic of the laser source.

(427 nm), and lattice defects related to oxygen and zinc vacancies (420 nm). The peak at 420 nm is also attributed to oxygen interstitial, however, based on theoretical predictions and other experimental results; it is more likely that oxygen interstitial is responsible for yellow emission [42,43]. Up to now, many researchers have demonstrated that the defects play a very important role and have strong influence on the sensing property of materials [44].

### 3.2. Measurements of sensing capabilities of the nanostructures

The adsorption of polar molecules on the surface of ZnO affects the surface potential and device characteristics. ZnO is an inorganic

metal oxide with amphoteric surface sites. These sites can protonate or deprotonate, leading to a surface charge and surface potential that is dependent on the electrolyte solution pH. This means that hydroxyl groups may act as proton donors or acceptors, depending on the electrolyte pH. The correspondence reactions are:

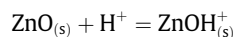
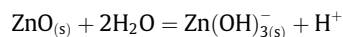
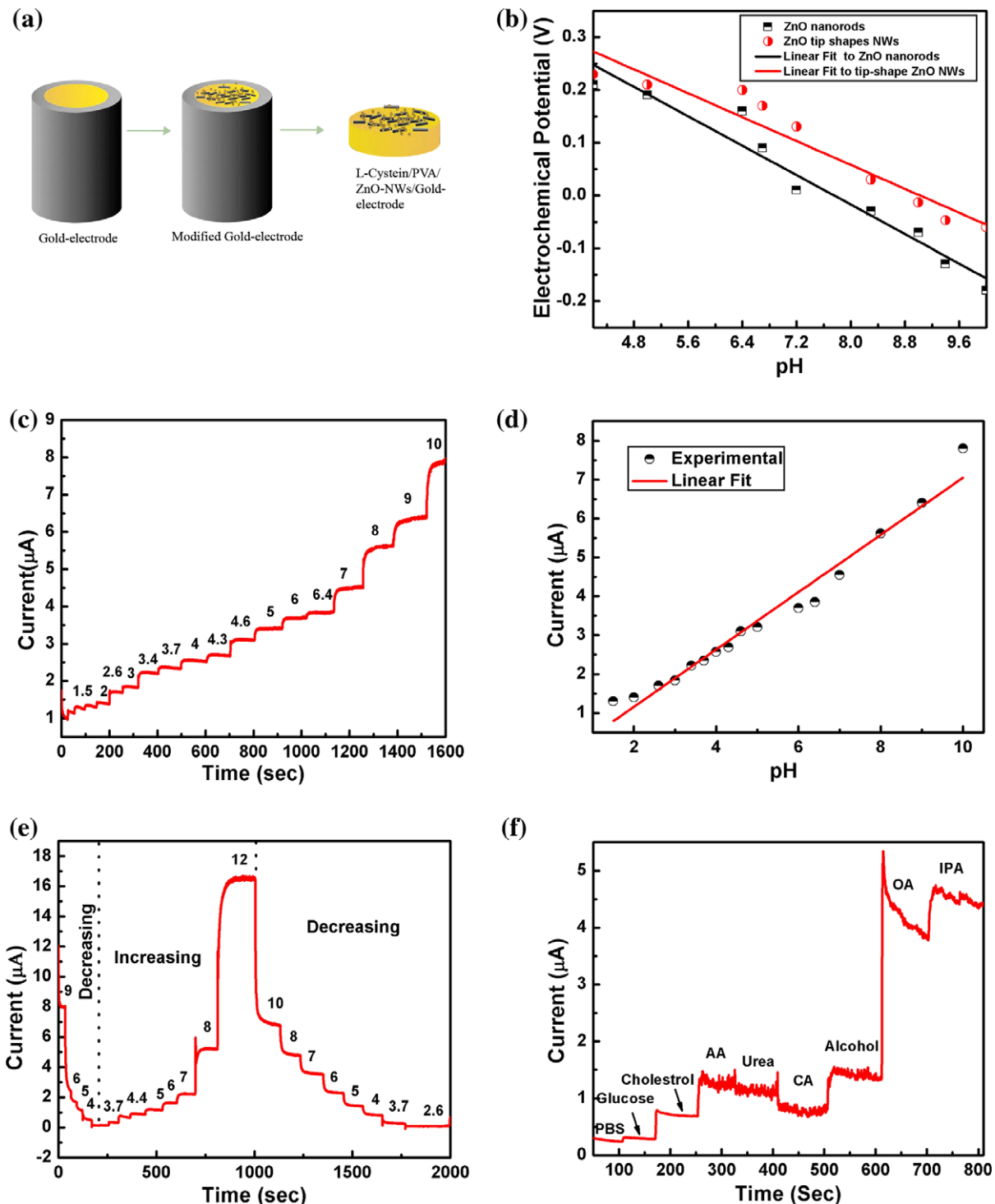


Fig. 4b shows the experimental evaluated surface potential response to the variation in pH of the electrolyte solution ranging from 4.2 to 10. It can be observed that the surface potential decreases with the increase in pH of the electrolyte. It can also observe that the pH sensitivity increases for tip-shape ZnO-NWs because of the shape edge and increase amount of defects in the NWs as shown in Fig. 3.

The sensing capabilities of the NWs have also been investigated by amperometric response of the modified electrode on the successive change of pH of the PB solution under continuously stirring at an applied potential of +0.5 V. The pH dependence of the modified electrode is evaluated in the range of pH 1.5–12 in this experiment. It can be seen from the Fig. 4c that the modified electrode exhibits a rapid and sensitive response to a series of solution whose pH is varied and an obvious increase in current can be seen corresponding to each value. The increase in current can be attributed to the increase in total surface charge density because of the combined acid and base behavior of both surface groups. A typical plot of the current response versus pH shows that the pH dependence is linear over the pH range 2–9 and thus suggests that ZnO-NWs could serve as a nanoscale pH sensors as shown in Fig. 4d. In addition, it is also observed that the current change is small at low pH range (2–5) but large at high pH range (6–10). The changes in current response are also reversible for increasing and decreasing pH



**Fig. 4.** (a) Schematic diagram of the modified gold electrode. (b) Experimental evaluated surface potential response under the variation in pH of the electrolyte solution. (c) Amperometric response of the modified electrode on the successive change of pH of the buffer solution under continuously stirring at an applied potential of +0.5 V. (d) A typical plot of evaluated current response versus pH. (e) Amperometric response of the modified electrode under the decrease and increase pH cycle of the buffer solution under continuously stirring at an applied potential of +0.5 V. (f) Amperometric response of the modified gold electrode to different electro-active species under consecutively added into continuously stirring 0.1 M PB solution (pH 7.0) at an applied potential of +0.5 V with a scan rate of  $0.1 \text{ V s}^{-1}$ .

as shown in Fig. 4e. It can be seen that the modified electrode shows very stable and fast response under each pH cycle.

To explore the bio-chemical sensing ability of the TSZONWs, a same quantity of electro-active species such as glucose, cholesterol, ascorbic acid (AA), urea, citric acid (CA), alcohol, oxalic acid (OA) and Isopropyl alcohol (IPA) are introduced into the PB solu-

tion. These species are consecutively added into continuously stirring PB solution and the current–time spectrum was obtained at an applied potential of +0.5 V with a scan rate of  $0.1 \text{ V s}^{-1}$ . It can be seen from Fig. 4f that the modified electrode shows well defined current response corresponding to each species. It has been observed that ZnO-NWs exhibit a small response when 0.5 mM urea

are added into the PB solution, while a decrease in current can be observed when citric acid is added. However, significant current increment can be observed when ascorbic acid (AA), oxalic acid and IPA are added. In addition, several experiments have been carried out to confirm that the observed current changes are due to the addition of bio-chemical species. By eliminating the ZnO-NWs from the gold electrode, we did not find any response corresponding to these species, confirming the role of ZnO-NWs as sensing the bio-chemical species in this particular case. All these results illustrate that the TSZONWs have also a good sensing ability for bio-chemicals species.

#### 4. Conclusion

In conclusion, we synthesized a bulk oriented arrays of tip-shape ZnO-NWs on the carbon nanotubes coated Si substrate where the carbon nanotubes play an important role for the synthesis of this structure. The tip-shape ZnO-NWs exhibit a large amount of defects which could lead to a significant role in the sensing applications. The biosensor based on TSZONWs is found to be very sensitive to the pH of the PB solution. To the best of our knowledge, this is the first time such a high and reproducible sensitivity has been achieved for pH sensor by using TSZONWs/gold modified electrode. In addition, the biosensor also shows the sensitivity of some bio-chemical species such as ascorbic acid, cholesterol etc. Hence, the sensing capabilities of TSZONWs could provide a new platform for others biosensor design and a potential future for clinical requirements.

#### Acknowledgment

This work is financially supported by National 973 Project of China and Chinese National Nature Science Foundation. The authors are grateful to the Higher Education Commission of Pakistan (HEC) for the financial support to Mashkooor Ahmad. The authors are also thanks to Miss Zhang Lei for assistance in making diagrams.

#### References

- [1] M.H. Huang et al., *Science* 292 (2001) 1897.
- [2] T. Aoki, Y. Hatanaka, D.C. Look, *Appl. Phys. Lett.* 76 (2000) 3257.
- [3] A. Bousfia, *Appl. Phys.* 87 (2000) 4507.
- [4] C.J. Lee, T.J. Lee, S.C. Lyu, Y. Zhang, H. Ruh, H.J. Lee, *Appl. Phys. Lett.* 81 (2002) 3648.
- [5] G. Sberveglieri, S. Groppelli, P. Nelli, A. Tintinelli, G. Giunta, *Sensors Actuat. B* 25 (1995) 588.
- [6] D.S. Ginley, C. Bright, *Mater. Res. Soc. Bull.* 25 (2000) 15.
- [7] W.E. Devaney, W.S. Chen, J.M. Stewart, R.A. Mickelsen, *IEEE Trans. Electron. Dev.* 37 (1990) 428.
- [8] W.P. Khang, C.K. Kim, *Sensors Actuat. B* 1314 (1993) 682.
- [9] A.H. Saffa, R. Al-Mofrarji, P. Klason, N. Gutman, A. Saar, A. Ost, P. Stralfors, M. Willander, *ENS 2007*, Paris, France, 2007.
- [10] G. Steinhoff, M. Hermann, W.J. Schaff, L.F. Eastmann, M. Stutzmann, M. Eickhoff, *Appl. Phys. Lett.* 83 (2003) 177.
- [11] J. Schallwig, G. Muller, M. Eickhoff, O. Ambacher, M. Stutzmann, *Sensors Actuat. B* 81 (2002) 425.
- [12] J.J. Wu, S.C. Liu, *Adv. Mater.* 14 (2002) 215.
- [13] S.C. Lyu, Y. Zhang, H. Ruh, H.J. Lee, H.W. Shim, E.K. Suh, C.J. Lee, *Chem. Phys. Lett.* 363 (2002) 134.
- [14] Z.L. Wang, X.Y. Kong, Y. Ding, P. Gao, W.L. Hughes, R. Yang, Y. Zhang, *Adv. Funct. Mater.* 14 (2004) 943.
- [15] P.D. Yang et al., *Adv. Funct. Mater.* 12 (2002) 323.
- [16] S. Iijima, *Nature* 354 (1991) 56.
- [17] K. Yu, Y.S. Zhang, F. Xu, Q. Li, Q. Li, Z.Q. Zhu, *Appl. Phys. Lett.* 88 (2006) 153123.
- [18] H. Kim, W. Sigmund, *Appl. Phys. Lett.* 81 (2002) 2085.
- [19] A. Chrissanthopoulos, S. Baskoutas, N. Bouropoulos, V. Dracopoulos, D. Tasis, S.N. Yannopoulos, *Thin Solid Films* 515 (2007) 8524.
- [20] B.S. Kang, F. Ren, Y.W. Heo, L.C. Tien, D.P. Norton, *Appl. Phys. Lett.* 86 (2005) 112105.
- [21] P.D. Batista, M. Mulato, *Appl. Phys. Lett.* 87 (2005) 143508.
- [22] R. Bashir, J.Z. Hilt, O. Elibol, A. Gupta, N.A. Peppas, *Appl. Phys. Lett.* 81 (2002) 3091.
- [23] A. Wei et al., *Appl. Phys. Lett.* 89 (2006) 123902.
- [24] J.S. Kim, W. Il Park, C.H. Lee, G.C. Yi, *J. Korean Phys. Soc.* 49 (2006) 1635.
- [25] N. Kumar, A. Dorfman, J. Hahm, *Nanotechnology* 17 (2006) 2875.
- [26] X. Cai, N. Klauke, A. Glidle, P. Cobbold, G.L. Smith, J.M. Cooper, *Anal. Chem.* 74 (2002) 908.
- [27] A. Wei et al., *Appl. Phys. Lett.* 89 (2006) 123902.
- [28] Y.T. Wang, L. Yu, Z.Q. Zhu, J. Zhang, J.Z. Zhu, C. Fan, *Sensors Actuat. B* 136 (2009) 332.
- [29] T. Kong, Y. Chen, Y. Ye, K. Zhang, Z. Wang, X. Wang, *Sensors Actuat. B: Chem.*, 2009, doi: 10.1016/j.snb.2009.01.002.
- [30] X.W. Sun, J.X. Wang, A. Wei, *J. Mater. Sci. Technol.* 24 (2008) 649.
- [31] R. Neuberger, G. Muller, O. Ambacher, M. Stutzmann, *Phys. Status Solidi A* 185 (2001) 85.
- [32] D.E. Yales, S. Levine, T.W. Healy, *J. Chem. Soc., Faraday Trans.* 70 (1974) 1807.
- [33] W.M. Siu, R.S.C. Collold, *IEEE Trans. Electron Dev.* ED-26 (1979) 1805.
- [34] L. Bousse, N.F. DeRooij, P. Bergveld, *IEEE Trans. Electron Dev.* ED-30 (1983) 1263.
- [35] C.D. Fung, P.W. Cheng, W.H. Ho, *IEEE Trans. Electron Dev.* ED-33 (1986) 8.
- [36] Y.C. Kong, D.P. Yu, B. Zhang, W. Fang, S.Q. Feng, *Appl. Phys. Lett.* 78 (2001) 407.
- [37] K. Vanheusden, W.L. Warren, C.H. Seager, D.K. Tallant, J.A. Voigt, B.E. Gnade, *J. Appl. Phys.* 79 (1996) 7983.
- [38] B.J. Jin, S. Im, S.Y. Lee, *Thin Solid Films* 366 (2000) 107.
- [39] X.L. Wu, G.G. Siu, C.L. Fu, H.C. Ong, *Appl. Phys. Lett.* 78 (2001) 2285.
- [40] S. Mahamuni, K. Borgohain, B.S. Bendre, V.J. Leppert, S.H. Risbud, *J. Appl. Phys.* 85 (1999) 2861.
- [41] J.Q. Hu, X.L. Ma, Z.Y. Xie, N.B. Wong, C.S. Lee, S.T. Lee, *Chem. Phys. Lett.* 344 (2001) 97.
- [42] B. Lin, Z. Fu, Y. Jia, *Appl. Phys. Lett.* 79 (2001) 943.
- [43] M. Lu, A.H. Kitai, P. Mascher, *J. Lumin.* 54 (1992) 35.
- [44] M.W. Ahn et al., *Appl. Phys. Lett.* 93 (2008) 263103.